Monitoring the reaction mechanism in model biogas reforming by *in situ* transient and steady-state DRIFTS measurements

Luis F. Bobadilla,[a]* Victoria Garcilaso, [a] Miguel A. Centeno, [a] and José A. Odriozola[a]*

Abstract: In this work, the reforming of model biogas reaction has been investigated on a $Rh/MgAl_2O_4$ catalyst. *In situ* transients and steady-state DRIFTS measurements were used to gain insights about the reaction mechanism involved in the activation of CH_4 and CO_2. It was found that the reaction proceeds through of an initial pathway in which methane and CO_2 are both dissociated on Rh metallic sites, and additionally a bifunctional mechanism in which methane is activated on Rh sites and CO_2 is activated on the basic sites of the support surface via formate intermediate by H-assisted CO_2 decomposition. Moreover, this plausible mechanism is able to explain why the observed apparent activation energy of CO_2 was much lower than that of CH_4. Our results suggest that the CO_2 dissociation facilitates the CH_4 activation because the oxygen adsorbed species formed in the decomposition of CO_2 are capable to react with the CH_x species derived from the methane decomposition.

Introduction

A key element to achieve a sustainable development is introducing renewable energy in the chemical production chain to reduce the impact on environment and greenhouse gas (GHG) emissions. The use of biomass (particularly waste) and reuse of CO_2 are two key elements enabling a new scenario for the chemical production [1]. Biogas generated by anaerobic digestion processes from the organic wastes is considered as one of the important bio-renewable resources for the next generation. The composition of biogas varies depending on the fermentation process and the feedstock, although the major constituents are methane (60%) and carbon dioxide (40%) with trace amounts of other gases [2]. Biogas reforming have received a great attention due to its environmental benefits from utilizing these two greenhouse gases and producing highly valuable synthesis gas (syngas, H_2 and CO) as a feedstock [3]. Syngas can be used as a raw material for the production of synthetic fuels with low environmental impact such as hydrogen, methanol, dimethylether (DME) and higher hydrocarbons [4].

Since model biogas is composed essentially by methane and carbon dioxide, the dry reforming of methane (DRM) is one of the more interesting reaction than can be applied to produce syngas:

$$\text{DRM: } CH_4 + CO_2 \rightarrow 2CO + 2H_2 \quad \Delta H = 247 \text{ kJ mol}^{-1} \qquad \text{(Eqn. 1)}$$

Several studies summarized in different reviews have showed the high efficiency of supported transition metals in this reaction [5]. Noble metals such as Rh, Ru, Pt, Pd and Ir are generally very active for DRM, without significant coke formation, due to small equilibrium constants for methane decomposition and low dissolution of carbon into their lattices [6]. Rh appears to be one of the most active and stable metals to catalyse CO_2 reforming of CH_4 [7]. It is generally accepted that the dissociative adsorption of both CH_4 and CO_2 on the metallic sites of the catalysts depend on both electronic and geometric factors. Evidence has been provided to indicate that differences in activity for DRM over a given metal dispersed on different supports may be due to metal–support interactions and/or the participation of O or OH species from the support in the metal–support interfacial region [5b]. As the adsorptive dissociation of methane, occurring on the metal surface, is one of the rate-limiting steps, the support must offer a high metal dispersion. Moreover, the support must provide the active sites for the adsorption and dissociation of CO_2. Wang and Ruckenstein [7b] reported that reforming rates on Rh-supported catalysts depend on the reducibility of the supports. Methane conversion on Rh supported non-reducible oxides (Al_2O_3, SiO_2, MgO, Y_2O_3, La_2O_3) is higher than on reducible ones (CeO_2, TiO_2). They concluded that MgO and Al_2O_3 are the most promising supports for CO_2 reforming of methane. On the other hand, it is well known that increased Lewis basicity of the support leads to increased adsorption of CO_2 which produces surface species able to react with carbon to form CO. For instance, it has been reported that the addition of MgO enhances the catalytic performance of alumina based catalysts as an effective promoter [8].

During the last decades, numerous studies have been devoted to understand the reaction mechanism and elementary steps at the atomic level of CO_2 dry reforming over noble metal supported catalysts [5a]. However, the nature of the adsorbed species involved in the process as well as the key intermediates remain still under debate. In order to know what exactly is occurring on the catalyst surface during the reaction it is necessary to combine the direct observation by spectroscopic techniques with the computational modelling methods. Recently, Polo-Garzón et al. have reported a complete mechanistic study employing *ab initio* methods [9] and steady-state isotopic transient kinetic analysis (SSITKA) [10] to gain insights into the dry reforming of methane reaction on Rh-substituted lanthanum zirconate pyrochlore catalyst. Combining both experimental and theoretical studies, they found that the main reaction pathway consists in the dehydrogenation of adsorbed methane to

[a] Dr. L.F.Bobadilla, V. Garcilaso, Dr. M.A. Centeno, Prof. J.A. Odriozola
Instituto de Ciencia de Materiales de Sevilla
Centro Mixto Universidad de Sevilla-CSIC
49 Av. Américo Vespucio, 41092 Sevilla (Spain)
E-mail: bobadilla@icmse.csic.es (Luis F. Bobadilla)
odrio@us.es (José A. Odriozola)

Supporting information for this article is given via a link at the end of the document

generate CH_2 species, which then are oxygenated to CH_2O species by atomic oxygen from CO_2 dissociation. CH_2O dehydrogenates to create CHO species, which undergoes dissociation to release a hydrogen atom and an adsorbed CO that later desorbs to yield product gas. These adsorbed hydrogens can also interact with surface bound species derived from CO_2 to yield additional CO product and water via the reverse water gas shift (RWGS) reaction. Erdöhelyi et al. [7c] investigated the CH_4 and CO_2 dissociation as well as the reforming reaction of CH_4 with CO_2 over Rh/Al_2O_3 by means of FTIR and kinetic measurements. They suggested that the CO_2 dissociation is promoted by the presence of methane. The products distribution depended strongly on the surface coverage by oxygen and carbon deposits.

In-situ transient diffuse reflectance infrared Fourier transform spectroscopy (DRIFTS) has been widely employed as a useful tool to elucidate the mechanism and uncover the role of the involved species during the reaction. However, the kinetic responses of the surface species analysed under transient conditions could be characteristically distinct from those measured from steady-state experiments. On the other hand, steady-state rate measurements cannot provide direct information about the nature and coverage of surface intermediates. Therefore, it would be desirable to integrate both transient and steady-state *in situ* approaches to gain a more comprehensive and definitive vision of the investigated catalytic reaction. A good understanding of the reaction mechanism will provide useful guidance to achieve an optimal catalyst in terms of activity, selectivity and durability. The present contribution deals with a comprehensive study to clarify some aspects of the activity of a Mg-promoted Rh/Al_2O_3 catalyst toward biogas reforming reaction and understand the mechanism using transient and steady-state DRIFTS experiments.

Results and Discussion

The activity of Rh supported on $MgAl_2O_4$ catalyst was measured under continuous flow-conditions at atmospheric pressure using a CH_4/CO_2 molar ratio equal to 1.5. Figure 1 depicts the influence of reaction temperature on CH_4 and CO_2 conversion, and on the H_2/CO molar ratio. It can be observed that both CH_4 and CO_2 conversion values increase with the temperature, in accordance with the strong endothermic character of the reaction. As CO_2 is the limiting reactant, it is expected that CH_4 conversion exhibit lower values for the whole temperature range compared to CO_2. The high conversion of CH_4 observed at higher temperatures could be ascribed to the methane decomposition reaction, as the predominant reaction to form hydrogen and carbon:

CH_4 decomposition: $CH_4 \leftrightarrow C + H_2 \quad \Delta H = 75\ kJ\ mol^{-1}$ (Eqn. 2)

Furthermore, this reaction could be favored by the secondary reaction of reverse water gas shift (RWGS), where the hydrogen produced is consumed in the reaction with CO_2 in agreement with results obtained by Parkhomenko et al. [11].

RWGS: $CO_2 + H_2 \leftrightarrow CO + H_2O \quad \Delta H = 41\ kJ\ mol^{-1}$ (Eqn. 3)

On the other hand, it is noticeable that the H_2/CO molar ratio values obtained increase with the increment of temperature and it becomes slightly greater than the stoichiometric value of 1 at 750 ºC. This fact could be explained by the dominance of the cracking reaction of CH_4 to form H_2 and carbon at higher temperatures. Moreover, according to thermodynamic equilibrium, for CH_4/CO_2 molar ratios superior to 1, the amount of H_2 produced increases with the temperature since CO_2 is the limiting reactant and the RWGS reaction cannot simultaneously improve along with the dry reforming reaction [12].

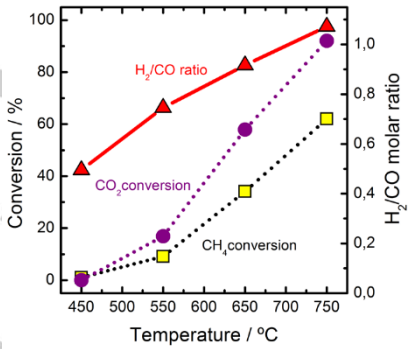

Figure 1. Effect of reaction temperature on the conversions of CO_2 and CH_4 and the molar ratio of H_2/CO over $Rh/MgAl_2O_4$ catalyst. Reaction conditions: WHSV = 150 L g^{-1} h^{-1}, CH_4/CO_2 = 1.5 and 1 bar

The results of catalytic activity presented in this study are in accordance with the thermodynamic model predicted by Nikoos et al. [13]. They reported that for CH_4/CO_2 molar ratio equal to 1.5, the methane decomposition reaction is considered to be the main reaction forming H_2 and carbon at higher temperatures.

In situ transient experiments were performed using two different combinations of reactants in order to observe the gas phase reactants and products and to identify the surface species present on the $Rh/MgAl_2O_4$ catalyst. We have examined the formation of surface species from gas streams containing CO_2 or H_2 + CO_2 at 600ºC, and subsequently, we have monitored the evolution of the formed species by switching a gas stream containing CH_4 every 560 s. Noteworthy that in this study we do not aim to identify which surface species are involved in H_2 production but rather to investigate the mechanism of CO_2 and CH_4 dissociation using DRIFTS as one of the most sensitive techniques for following the interaction of CO_2 and/or CH_4 with the catalyst. This type of experiment enables direct correlation of specific surface species with the production of gaseous products.

A series of IR spectra recorded during alternate switching between CO_2 and CH_4 feeds are presented in Fig.2A. The IR features obtained during CO_2 exposure show that adsorption of CO_2 at 600 °C leads to the formation of metallic carbonyls and CO adsorbed species as well as to CO gas-phase. This fact

reveals that CO_2 adsorption dissociative takes place on the surface catalyst and more concretely on the metallic active sites. In addition, the rhodium-based catalyst presents several bands in the range 1350-1650 cm^{-1} that can be ascribed to carbonate species. It is generally accepted that CO_2 chemisorption and dissociation on a transition metal surface is dominated by electron transfer and requires the formation of a carbonate precursor [14]. When CO_2 stream was switched by CH_4 stream, the IR bands attributed to carbonates species almost disappeared completely while that the intensities of the bands attributed to CO adsorbed and metallic carbonyls were only partially decreased.

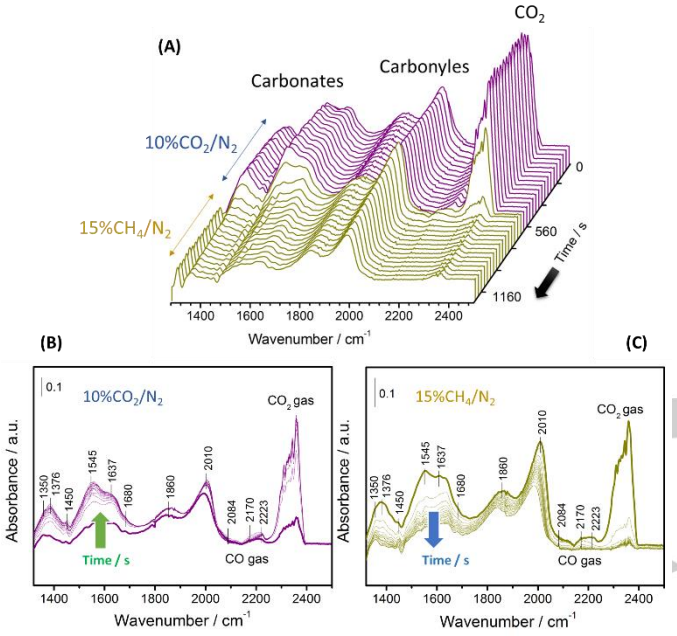

Figure 2. DRIFT spectra collected at 650ºC when the feed gas was switched from CO_2/N_2 to CH_4/N_2 over $Rh/MgAl_2O_4$ catalyst.

The temporal evolution of the bands attributed to the different species can be seen more clearly in Fig. 2B and Fig. 2C. The bands appearing at 1450-1680, 1376-1545 and 1350-1637 cm^{-1} can be assigned to three types of carbonates surface adsorbed species on the Rh supported catalyst: bicarbonate, monodentate and bidentate carbonates, respectively [15]. The different CO_2 adsorption modes depend on the chemical nature of the surface oxygen atoms. The chemisorption of CO_2 reveals acidic sites where the CO_2 molecule preserves its linear geometry upon adsorption, and basic sites as well as acid-base pairs when carbonate-likes species are formed [15a]. Monodentate carbonates formation involves low-coordination or isolated surface O_2^- anions such as those present in corners or edges, bidentate carbonate forms on Lewis-acid–base pairs ($M\text{-}O_2^-$ pair site, where M is the metal cation Mg or Al), and bicarbonate formation involves surface hydroxyl groups [15d, 16]. CO adsorbed on Rh-based catalysts has been widely investigated and different CO species can be present. The IR bands at 2010 and 1860 cm^{-1} can be attributed to linear and bridged adsorbed CO species on Rh metallic sites, respectively [17]. There is also a weaker feature at 2084 cm^{-1} that can be assigned to a germinal (*gem*-) dicarbonyl species [18]. The presence of *gem*-dicarbonyl species is associated to de the oxidation of Rh^0 to Rh^+ cations due to the presence of hydroxyl groups on the support surface according to [19]:

$$2Rh + 4CO + 2Al(Mg)OH \rightarrow H_2 + 2Al(Mg)\text{-}O\text{-}Rh(CO)_2 \quad \text{(Eqn. 4)}$$

This oxidation disrupts the Rh-Rh bonds generating the *gem*-dicarbonyl species and provoking a redispersion of the Rh particles [20]. Thus, the detection of *gem*-dicarbonyl complexes is considered significant for the existence of highly dispersed Rh metal particles on the catalyst surface. Apart from this, it is noticeable a broad feature in the 2100-2250 cm^{-1} region which correspond to CO gas (inside the cell) and two weak peaks at 2170 and 2223 cm^{-1} that can be assigned to CO adsorbed to low coordinated Al^{3+} ions on the $MgAl_2O_4$ spinel structure and alumina support, respectively [21].

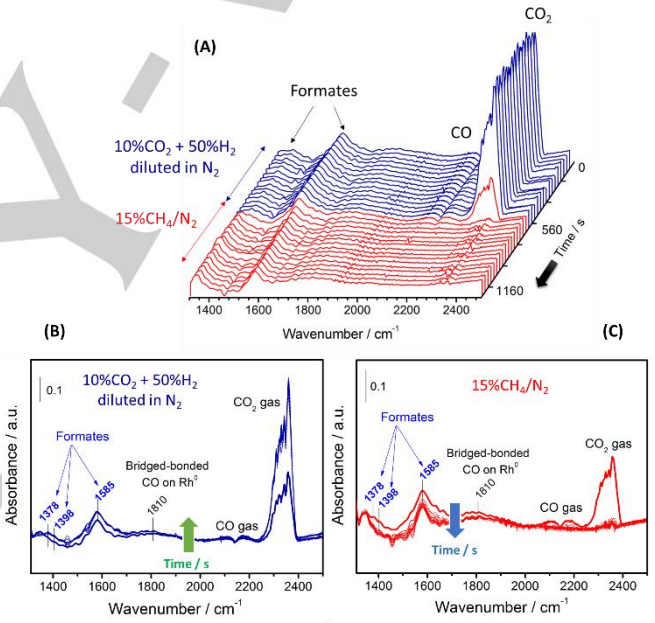

Figure 3. DRIFT spectra collected at 650ºC when the feed gas was switched from $(CO_2+H_2)/N_2$ to CH_4/N_2 over $Rh/MgAl_2O_4$ catalyst.

A series of spectra reported in Fig. 3A shows the evolution of the surface species formed on the $Rh/MgAl_2O_4$ catalyst during alternate switching between $CO_2 + H_2$ (1:4 molar ratio) and CH_4-only feeds. During the $CO_2 + H_2$ introduction, compared with the CO_2 exposure (Fig. 2A), the appearance of new IR features at 1580, 1398 and 1378 cm^{-1} as well as a low intense band at 2915 cm^{-1} (not shown) indicates the presence of adsorbed formate species on the catalyst surface. Moreover, the formation of gas-phase CO reveals that RWGS reaction takes place. As has been claimed in the literature, it is assumed that the formation of CO proceeds via decomposition of formate species as intermediates in the RWGS reaction. On the other hand, it can be also observed the presence of CO-bridged adsorbed species. The

CO produced by RWGS reaction can interact with the Rh particles forming CO linear, CO bridged and/or *gem*-dicarbonyl species. The only presence of CO-bridged species suggests their inactivity and its possible role as spectator during the reaction.

Figure 4 illustrates the concentration profiles of CO_2 and CH_4 during the modulation of both combination of reactants, CO_2 vs CH_4 and CO_2 + H_2 vs CH_4, for a period of 3 modulation cycles. As can be noticed, when only CO_2 was exposure the concentration of CO_2 was gradually increased until the CO_2 saturation level was reached. According to the DRIFTS results discussed above (Figure 2), it is evident that CO_2 is dissociated to CO and oxygen active species during an initial transient or induction period where the metallic surface particles become entirely covered of CO-adsorbed species and at the same time CO_2 is trapped over the surface support on the basic adsorption sites expectedly in the form of surface carbonates. Subsequently, by switching the gas feed from CO_2 to CH_4, the oxygen active species on metallic sites favored the CH_4 decomposition to H_2 and CH_x species and the concentration of methane delays a few of seconds to achieve the saturation level. On the other hand, during the CO_2 + H_2 mixture feed, one may notice that the level of CO_2 in the effluent was always below the saturation level reveling a continuous formation of CO via RWGS reaction. As the gas stream was switched to methane, the level of methane directly reached the saturation without the ongoing increase during the initial several seconds. This reveals the absence of active oxygen species capable to activate the CH_4 dissociation since in presence of hydrogen predominates the H-assisted CO_2 dissociation to produce CO via formate intermediates.

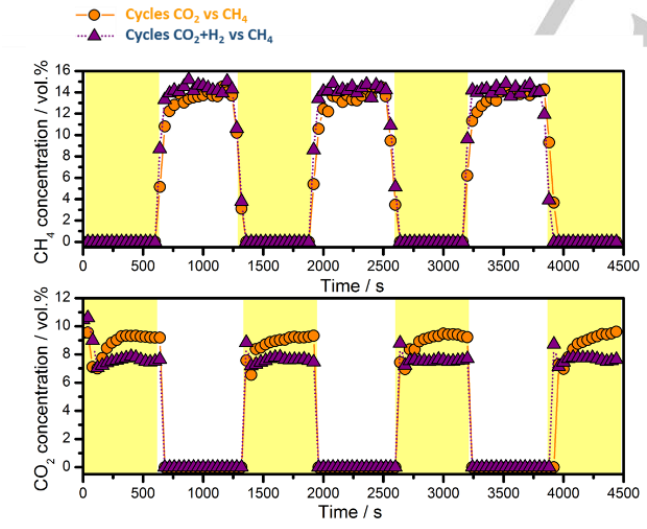

Figure 4. CH_4 and CO_2 concentration profiles as a function of time when the feed gas was switched from H_2/N_2 or $(CO_2+H_2)/N_2$ to CH_4/N_2 over $Rh/MgAl_2O_4$ catalyst at 650ºC.

On the basis of the above understanding, two possibilities could be considered for the production of CO: i) direct dissociation of CO_2 on Rh metallic particles in absence of hydrogen, and ii) H-assisted CO_2 reduction by dehydroxylation of intermediate formate species formed on the support. Concerning to the former possibility, we have observed that carbon dioxide dissociation is achieved in absence of hydrogen and a large amount of CO adsorbed species on Rh is produced. By contrast, the H-assisted carbon monoxide formation can be assumed to occur through an activated formate-type intermediates, which accounts for the amount of formate species on the catalyst surface.

In absence of hydrogen, our data show the activation of CO_2 on Rh catalyst occur via direct dissociation to CO adsorbed and O. When methane is introduced, the adsorbed oxygen facilitates the dissociation of methane by reaction with the CH_x formed on the catalyst surface. In opposite, the H-assisted activation of CO_2 produces formate species adsorbed that decompose to CO and H_2O. The absence of active oxygen species on the metal surface in this case enables the activation of methane and only RWGS reaction is possible. Thus, one can conclude that the CO_2 dissociation results in the covering of the metallic sites with adsorbed active oxygen species which favors the methane dissociation.

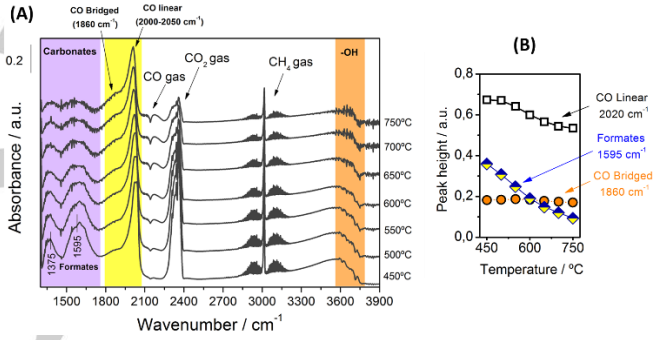

Figure 5. (A) DRIFT spectra obtained during CO_2 reforming of methane in the temperature range from 450 to 750ºC. **(B)** Evolution of the peak height attributed to CO-linear, CO-bridged and formate surface species as a function of the reaction temperature. Reaction conditions: 1 bar, total flow rate of 50 mL min^{-1} and CH_4/CO_2 = 1.5 (molar ratio).

In situ DRIFTS spectroscopy was used to study the chemical nature of intermediate species formed during the biogas reforming reaction in the temperature range of 450–750 ºC on the $Rh/MgAl_2O_4$ catalyst. Figure 5A shows the DRIFTS spectra recorded under steady-state conditions for the $Rh/MgAl_2O_4$ catalyst after stabilization under the reaction mixture at the indicated temperature. The spectra recorded at every temperature present intense bands ascribed to absorbed carbonyls with peaks around 1860 and in the range 2000-2050 cm^{-1} range corresponding to linear and bridged carbonyls on metallic rhodium, respectively, while the IR bands in the 1300-1650 cm^{-1} range signify carbonate species [15a]. Furthermore, it can be appreciated the presence of intense bands at 1590-1375 cm^{-1} corresponding to formates [15b]. Fig. 5B reports a plot of the height peaks associated with surface formates (1595 cm^{-1}), CO-bridged (1860 cm^{-1}) and CO-linear (2020 cm^{-1}) as a function of the reaction temperature. As can be observed, by increasing the reaction temperature the amount of formate species is notably

decreased while that of linearly adsorbed CO species are slightly decreased and the content of bridged carbonyls remains unaltered. This suggest that the bridged adsorbed CO species are spectator during the reaction. It can be understood considering that the Rh-CO bonding in bridged carbonyls is much more stable and stronger than in linear carbonyls and *gem*-dicarbonyls.

The turnover frequency (TOF) can be defined as the number of product molecules produced or the number of reactant molecules transformed per catalyst site and per unit time. The most common manner to determine the TOF is from the relationship between the reaction rate and the surface metal exposed. The calculation of TOF is complicated since it is impossible to know exactly the real number of accessible active sites under reaction conditions. Moreover, it depends on whether the reaction is structure-sensitive or structure-insensitive. Thus, the quantification of the exact number of surface sites exposed requires an approximation [22]. Although it is well known that both the methane activation and the dissociation of CO_2 are structure sensitive and promoted at defect sites such as edges and corners [5b], we have assumed that all the surface atoms of Rh exposed are active sites in the main reaction pathway. We suppose that if they are not all equally active, the turnover rate will have an average value. Accordingly, the TOF was calculated by using the following equation [23]:

$$TOF = \frac{r \cdot M_{Rh}}{D_{Rh}} \; [s^{-1}]$$

where r is the reaction rate expressed in $mol_{reactant\ converted}\ mol_{Rh}^{-1}\ s^{-1}$, M_{Rh} is the atomic weight of rhodium (102.9 g mol^{-1}) and D_{Rh} is the metal dispersion. In all cases, rhodium dispersion was estimated to be 85 % on the basis of the cuboctahedral particles model proposed by Polisset [24] and assuming an average Rh particle size of 1 nm obtained by TEM measurements (Fig. S2 in Supporting Information). The reaction rates of CO_2 and CH_4 converted were estimated from the data analysis of gas-phase in the DRIFTS cell.

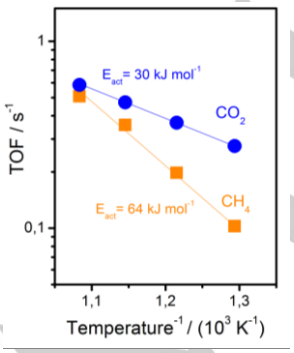

Figure 6. Turnover frequencies (TOFs) of CO_2 and CH_4 consumption as a function of reciprocal temperature expressed in Kelvin units on $Rh/MgAl_2O_4$ obtained in the DRIFTS cell. Reaction conditions: 1 bar, total flow rate of 50 mL min^{-1} and CH_4/CO_2 = 1.5 (molar ratio).

Figure 6 shows the CH_4 and CO_2 turnover rates (TOFs) plotted against reciprocal temperature expressed in Kelvin units in order to estimate the apparent activation energy. As can be observed, the apparent activation energy of CO_2 consumption (30 kJ mol^{-1}) was much lower than that of CH_4 one (64 kJ mol^{-1}). Similar values of activation energy for CH_4 and CO_2 were obtained by Zhang et al. [25] using a bimetallic Ni-Co/Mg(Al)O catalyst. This points to the important influence of the support in the reaction and likely this notably difference between activation energies of CO_2 and CH_4 was due to the presence of strong Lewis basic sites on $MgAl_2O_4$ spinel, which facilitates the CO_2 activation. On the other hand, the presence of formate species observed by *in situ* DRIFTS indicates that RWGS reaction plays a major role in the CO_2 activation and the support has an important influence in the reaction mechanism. This observation is in agreement with the results reported by Nagaoka et al. [26] for Pt-based catalysts, where the activation energy for the rate of CH_4 and CO_2 disappearance varies for different supports. The majority of values reported in the literature using different noble metals as active phase shows that the activation energy for methane is greater than the one estimated for CO_2. This is consistent with other reactions involving methane and it is mainly due to the high energy required to activate the stable C-H bond on methane.

Most of the reaction mechanism reported in the literature for the CO_2 reforming of methane reaction are based on the Langmuir-Hinshelwood model. It involves a dissociative adsorption of the reactants (CH_4 and CO_2) followed by rate-determining surface reaction of the adsorbed species to the final products [27]. Based on the results obtained in this work and the reaction mechanisms postulated in the literature, the following elementary reaction steps seem appropriated to describe the mechanism involved in the biogas reforming reaction:

1) **CO_2 (g)** ↔ CO* + O* CO_2 direct dissociation
2) **CH_4 (g)** ↔ CH_3* + H* CH_4 dissociation on metal
3) CH_3* ↔ CH_2* + H*
4) CH_2* ↔ CH* + H*
5) CH* ↔ C* + H*
6) H* + H* ↔ **H_2(g)** H_2 desorption
7) **CO_2 (g)** ↔ CO_2* CO_2 adsorption as carbonates
8) CO_2* + H* ↔ COOH* H-assisted CO_2 activation
9) COOH* ↔ CO* + OH*
10) CH* + O* ↔ COH* Oxidation of CH_x fragments

11) $CHO^* \leftrightarrow CO^* + H^*$

12) $CO^* \leftrightarrow \mathbf{CO\ (g)}$ Desorption of CO

13) $OH^* + H^* \leftrightarrow H_2O^*$

14) $H_2O^* \leftrightarrow \mathbf{H_2O\ (g)}$ Desorption of H_2O

Here, (*) correspond to an adsorption site on the catalyst surface. Among these steps, methane dissociation could be considered the rate-determining steps in the reforming reaction since it is necessary to activate the stable C-H bond [28]. Figure 7 shows an illustrative representation of the steps than can be tentatively involved in the reaction mechanism of the model biogas reforming. In a first step where the support plays a minor role, the dissociative adsorption of methane on metal Rh sites produces hydrogen and CH_x species whereas CO_2 is also adsorbed dissociatively on the metallic particles to form CO and O. Then, this oxygen adsorbed species reacts with CH_x and leads to formation of CH_xO species. Finally, the CH_xO species then dissociates to form CO and H_2 in a fast step. We can assume that the CO_2 dissociation facilitates the CH_4 activation by oxygen adsorbed formed in the decomposition of CO_2. Besides we believe that the formation of oxygen species provokes a partial oxidation of the Rh metallic particles. As we mentioned above, this oxidation disrupts the Rh-Rh bonds generating the *gem*-dicarbonyl species and provoking a redispersion of the Rh particles. Likely this gem-dicarbonyl species are unstable and rapidly are transformed to bridged CO species. On the other hand, the hydrogen generated in the first step initiates a new bifunctional mechanism in which two types of active centers, basic sites of support and metallic particles, are involved in the reaction pathway where the role of the support is crucial. The CO_2 is adsorbed on the basic sites of the support to form carbonates/bicarbonates species that subsequently are transformed to CO and H_2O via formation of formate-type intermediates by H-assisted CO_2 decomposition. The later process participates in the reaction mechanism through the RWGS reaction and it is obvious that the formation of formate species requires a close vicinity of the carbonate species and the metal adsorbed hydrogen. Therefore, the formation of formate species proceeds mainly at the metal-support interface although they can migrate to the surface support where they are stably adsorbed and detected by DRIFTS [29].

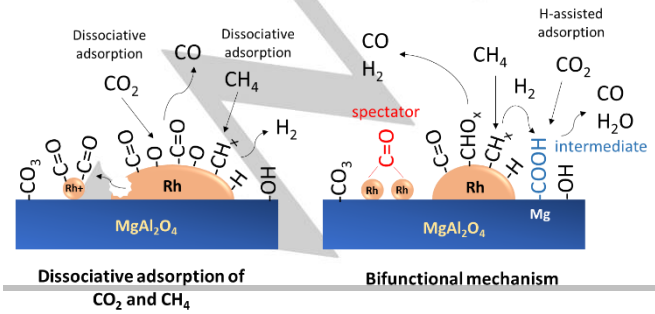

Figure 7. Schematic representation of the plausible reaction mechanism for model biogas reforming over $Rh/MgAl_2O_4$ catalyst.

The majority of the reaction mechanism postulated in the literature for different supported catalysts, except those developed for inert supports, are based on bifunctional pathway. This bifunctional pathway is widely accepted, with the reaction taking place on catalysts with active metal and support having either electrophilic or nucleophilic character. For active metals on inert supports, the metal catalyzes all the surface reactions and is more prone to deactivation due to carbon deposition or sintering [5a].

Conclusions

On the basis of *in situ* transient and steady-state DRIFTS studies, a reaction mechanism focused on the activation of CO_2 and CH_4 on $MgAl_2O_4$-supported Rh catalyst was proposed for the model biogas reforming reaction. It was found that dissociative adsorption of CO_2 takes place initially and the active oxygen species formed on the metallic sites facilitates the CH_4 activation. The hydrogen generated in this first step initiates a new bifunctional mechanism in which CO_2 is activated on the basic sites of the support surface via formate intermediate by H-assisted CO_2 decomposition. Therefore, CO_2 can be transformed into CO through two pathways: CO_2 direct dissociation on metallic sites and H-assisted dissociation on metal-support interface.

Experimental Section

Rh (1 wt.% nominal) supported over $MgAl_2O_4$ catalyst was prepared by impregnation using the incipient wetness method. For the support synthesis, γ-alumina (Spheralite SCS505) sieved between 100-200 μm was impregnated with an alcoholic solution of $Mg(NO_3)_2{\cdot}6H_2O$ (28 wt.% of MgO). It should be mentioned that the theoretical amount of MgO required to completely transform the alumina into the "ideal" spinel phase is ca. 28 wt.% [30]. Further, the solid was dried overnight at 100 ºC and then calcined in air 24h at 900 ºC. Regarding the active phase impregnation, an aqueous solution of $Rh(NO_3)_3{\cdot}2H_2O$ was impregnated over the support and it was dried and calcined in air at 500 °C for 8 h (2 ºC min^{-1}). The elemental composition of the catalyst was determined by ICP analysis. Textural properties, phase structure and morphology of the catalyst were investigated by nitrogen adsorption/desorption isotherms at liquid nitrogen temperature, powder X-ray diffraction and transmission electron microscopy, respectively. Further details on the catalyst characterization are described in the Supporting Information.

The dry reforming activity of the catalyst was measured in a fixed bed continuous-flow reactor working at atmospheric pressure using a commercial Microactivity Reference® equipment. The amount of catalyst used was 50 mg diluted in crushed quartz both sieved in the 100–200 μm range. Prior to reaction, the catalyst was reduced at 750 °C for 3 h in a

100 mL min^{-1} H_2 (50 vol.% in N_2) stream. The CH_4/CO_2 mixture, with molar ratio maintained at 1.5 simulating a model biogas, was passed through the reactor at a total flow rate of 167 ml min^{-1} (WHSV = 150 L g^{-1} h^{-1}) and the reaction temperatures were maintained at 450, 550, 650 and 750 °C in a tubular furnace. A thermocouple was placed into the center of the catalyst bed to record the reaction temperature and to control the furnace. Gas products were analyzed on line using a microGC (Varian 4900) equipped with Porapak Q and MS-5A columns. The conversions of CH_4 and CO_2 were calculated based on the difference between the input and output of CH_4 and CO_2, respectively.

In-situ DRIFTS measurements were carried out using a high temperature environmental reaction chamber supported in a Praying Mantis (*Harrick*) DRIFTS optical system with ZnSe windows. The spectra were collected using a Thermo Nicolet Nexus FT-IR spectrometer equipped with a liquid nitrogen cooled MCT detector at 4 cm^{-1} resolution and average of 64 scans. The whole optical path was purged with CO_2- and H_2O-free nitrogen. About 50 mg of catalyst finely ground was loaded in the cell for each measurement. The gases pass through the catalyst packed-bed, mimicking the plug-flow condition of the reaction. Different mixtures of gases could be introduced into the cell, and the gas flows were controlled by mass-flow controllers from AALBORG appropriately calibrated. All the valves, connexions and pipelines of the reaction system were heated at 100 ºC to prevent the water condensation produced during the reaction. Prior to the measurements, the catalyst was activated *in situ* at 750 ºC in 50% H_2/N_2 in a total flow rate of 50 mL min^{-1}.

For the transient experiments, the different mixtures at a total flow rate of 50 mL min^{-1} (10% CO_2 diluted in N_2, 15% CH_4 diluted in N_2, 40% H_2 + 10% CO_2 diluted in N_2) were switched and introduced into the IR cell under isothermal conditions at 600ºC every 560 s. A four-way valve was installed to allow us to switch between two gas mixtures. The experiment of steady-state was performed feeding into the IR cell a mixture of 15% CH_4 and 10% CO_2 in nitrogen balance for a total flow rate of 50 mL min^{-1}. The temperature range used varies from 450 to 750 °C with stepwise at 50 °C intervals and remaining at each temperature for 30 min in order to obtain steady-state conditions. The concentration of CO_2 was monitored by time-resolved analysis using a VAISALA CO_2 measurement meter. The concentration of CH_4 was estimated by integration of the band area of ν_{as} (C-H) attributed to gas phase methane (3015 cm^{-1}). A previous calibration by flowing CH_4/N_2 mixtures over α-Al_2O_3 at different temperatures was performed to obtain the relationship between the band area of ν_{as} (C-H) and the partial pressure of methane inside the cell. In the temperature range used, no reaction between methane and α-Al_2O_3 was observed, although the thermal effect must be considered. As temperature increases, the intensity of gaseous compounds DRIFTS signal decrease. With this kind of calibration, absorption coefficients can be estimated, and product quantitative analysis can be made in catalytic tests. This one, for instance, has been used in CO and CO_2 methanation reactions over Rh-supported catalysts [31].

Acknowledgements

Financial support for this work has been obtained from the Spanish Ministerio de Economía y Competitividad (MINECO) (ENE2013-47880-C3-2-R and ENE2015-66975-C3-2-R) and from Junta de Andalucía (TEP-8196). Victoria Garcilaso ackowledges MINECO by their FPI fellowship (BES-2013-062806).

Keywords: Biogas reforming • Reaction mechanism • *In situ* transient DRIFTS

[1] S. Perathoner, G. Centi, *ChemSusChem* **2014**, *7*, 1274-1282.
[2] S. Zinoviev, F. Müller-Langer, P. Das , N. Bertero , P. Fornasiero , M. Kaltschmitt , G. Centi , S. Miertus, *ChemSusChem* **2010**, *3*, 1106-1133.
[3] aV. P. Rathod, J. Shete, P. V. Bhale, *Int. J. Hydrogen Energy* **2016**, *41*, 132-138; bP. Djinović, I. G. O. Črnivec, A. Pintar, *Catal. Today* **2015**, *253*, 155-162; cV. Chiodo, A. Galvagno, A. Lanzini, D. Papurello, F. Urbani, M. Santarelli, S. Freni, *Energy Conv. Manag.* **2015**, *98*, 252-258.
[4] A. Vita, L. Pino, F. Cipitì, M. Laganà, V. Recupero, *Fuel Process. Technol.* **2014**, *127*, 47-58.
[5] aD. Pakhare, J. Spivey, *Chem. Soc. Rev.* **2014**, *43*, 7813-7837; bM. C. J. Bradford, M. A. Vannice, *Catal. Rev. Sci. Eng.* **1999**, *41*, 1-42; cC. Papadopoulou, H. Matralis, X. Verykios, in *Catalysis for Alternative Energy Generation* (Eds.: L. Guczi, A. Erdôhelyi), Springer New York, New York, NY, **2012**, pp. 57-127; dB. C. Enger, R. Lødeng, A. Holmen, *Int. J. Hydrogen Energy* **2012**, *37*, 10418-10424.
[6] aY. H. Hu, E. Ruckenstein, in *Adv. Catal., Vol. Volume 48*, Academic Press, **2004**, pp. 297-345; bJ. R. Rostrup-Nielsen, J. H. B. Hansen, *J. Catal.* **1993**, *144*, 38-49; cJ. Wei, E. Iglesia, *J. Phys. Chem. B* **2004**, *108*, 4094-4103.
[7] aJ. Wei, E. Iglesia, *J. Catal.* **2004**, *225*, 116-127; bH. Y. Wang, E. Ruckenstein, *Appl. Catal. A Gen.* **2000**, *204*, 143-152; cA. Erdöhelyi, J. Cserenyi, F. Solymosi, *J. Catal.* **1993**, *141*, 287-299.
[8] L. Zhang, Q. Zhang, Y. Liu, Y. Zhang, *Appl. Surf. Sci.* **2016**, *389*, 25-33.
[9] F. Polo-Garzón, M. He, D. A. Bruce, *J. Catal.* **2016**, *333*, 59-70.
[10] F. Polo-Garzón, D. Pakhare, J. J. Spivey, D. A. Bruce, *ACS Catal.* **2016**, *6*, 3826-3833.
[11] K. Parkhomenko, A. Tyunyaev, L. M. Martinez Tejada, D. Komissarenko, A. Dedov, A. Loktev, I. Moiseev, A.-C. Roger, *Catal. Today* **2012**, *189*, 129-135.
[12] N. D. Charisiou, G. Siakavelas, K. N. Papageridis, A. Baklavaridis, L. Tzounis, D. G. Avraam, M. A. Goula, *J. Natural Gas Sci. Eng.* **2016**, *31*, 164-183.
[13] M. K. Nikoo, N. A. S. Amin, *Fuel Process. Technol.* **2011**, *92*, 678-691.
[14] F. Solymosi, *J. Mol. Catal.* **1991**, *65*, 337-358.
[15] aC. Morterra, G. Ghiotti, F. Boccuzi, S. Coluccia, *J. Catal.* **1978**, *51*, 299-313; bF. Solymosi, A. Erdöhelyi, M. Kocsis, *J. Catal.* **1980**, *65*, 428-436; cY.-G. Chen, K. Tomishige, K. Yokoyama, K. Fujimoto, *J. Catal.* **1999**, *184*, 479-490; dD. Li, R. Li, M. Lu, X. Lin, Y. Zhan, L. Jiang, *Appl. Catal. B Environ.* **2017**, *200*, 566-577; eJ. I. Di Cosimo, V. K. Díez, M. Xu, E. Iglesia, C. R. Apesteguía, *J. Catal.* **1998**, *178*, 499-510.
[16] M. A. Al-Daous, A. A. Manda, H. Hattori, *J. Mol. Catal. A Chem.* **2012**, *363–364*, 512-520.
[17] aC. M. Carbonell, C. O. Areán, *Vib. Spectrosc.* **1996**, *12*, 103-107; bM. Cavers, J. M. Davidson, I. R. Harkness, L. V. C. Rees, G. S. McDougall, *J. Catal.* **1999**, *188*, 426-430.
[18] S. Trautmann, M. Baerns, *J. Catal.* **1994**, *150*, 335-344.
[19] F. Solymosi, M. Pasztor, *J Phys. Chem.* **1985**, *89*, 4789-4793.
[20] P. Malet, J. J. Benitez, M. J. Capitan, M. A. Centeno, I. Carrizosa, J. A. Odriozola, *Catal. Lett.* **1993**, *18*, 81-97.
[21] aC. M. Carbonell, C. O. Areán, *Vibr. Spectrosc.* **1996**, *12*, 103-107; bE. Finocchio, G. Busca, P. Forzatti, G. Groppi, A. Beretta, *Langmuir* **2007**, *23*, 10419-10428.
[22] M. Boudart, *Chem. Rev.* **1995**, *95*, 661-666.
[23] T. R. Reina, S. Ivanova, J. J. Delgado, I. Ivanov, V. Idakiev, T. Tabakova, M. A. Centeno, J. A. Odriozola, *ChemCatChem* **2014**, *6*, 1401-1409.
[24] M. Polisset, University of Paris VI **1990**.
[25] J. Zhang, H. Wang, A. K. Dalai, *Ind. Eng. Chem. Res.* **2009**, *48*, 677-684.
[26] K. Nagaoka, K. Seshan, J. A. Lercher, K.-i. Aika, *Catal. Lett.* **2000**, *70*, 109-116.

[27] Y. Kathiraser, U. Oemar, E. T. Saw, Z. Li, S. Kawi, *Chem. Eng. J.* **2015**, *278*, 62-78.
[28] A. C. Luntz, J. Harris, *Surf. Sci.* **1991**, *258*, 397-426.
[29] D. Heyl, U. Rodemerck, U. Bentrup, *ACS Catal.* **2016**, *6*, 6275-6284.
[30] A. Penkova, L. Bobadilla, S. Ivanova, M. I. Domínguez, F. Romero-Sarria, A. C. Roger, M. A. Centeno, J. A. Odriozola, *Appl. Catal. A Gen.* **2011**, *392*, 184-191.
[31] J. J. Benítez, I. Carrizosa, J. A. Odriozola, *Appl. Spectrosc.* **1993**, *47*, 1760-1766.

FULL PAPER

Understanding the mechanism: The production of syngas from biogas represents an attractive approach for reducing greenhouse emissions. We contribute to gain a better understanding of the reaction mechanism in the biogas reforming for developing more economic and efficient catalysts.

Luis F. Bobadilla, Victoria Garcilaso, Miguel A. Centeno and José A. Odriozola**

Page No. – Page No.

Monitoring the reaction mechanism in model biogas reforming by *in situ* transient and steady-state DRIFTS measurements